

Two-dimensional model for femtosecond laser ablation of metals: validation with percussion drilling experiments

Pol Vanwersch^{1,2,3}, Tim Evens², Albert Van Bael², Sylvie Castagne¹

¹KU Leuven, Department of Mechanical Engineering and Flanders Make @KU Leuven-MaPS

²KU Leuven, Department of Materials Engineering, Diepenbeek Campus, Belgium

³FWO Research Foundation Flanders, Brussels, Belgium

pol.vanwersch@kuleuven.be

Abstract

Femtosecond (fs) laser ablation of metals is gaining popularity in surface texturing and micro-machining applications thanks to its high precision and negligible heat affected zone. However, the wide variety of phenomena influencing the ablation, as well as the non-linear nature of the process, makes finding the adequate laser parameters a difficult task. A model can be used to predict the outcome of the laser ablation process and thus to reduce the experimental costs linked to the research of the optimal process parameters to create a desired geometry. Femtosecond laser ablation can be represented by the two-temperature model, where, due to the very short pulse duration (shorter than the electron-phonon relaxation time), a difference between the temperature of the electrons excited by the laser pulse and the temperature of the lattice is assumed. This two-temperature model has been used to predict the ablation profiles created by percussion drilling in a low corrosion tool steel. In this paper, we present the validation of this modelling approach for percussion drilling with a circularly polarized laser beam. The model is first fitted with material parameters found in the literature, then the material parameters are modified to generate an optimal match with the experimental results. Micro-computer tomography was used for the experimental analysis of the ablated geometries. The results show a good overall correspondence between the simulation and the experimental data.

Femtosecond laser modelling, ultrafast laser ablation, percussion drilling

1. Introduction

Femtosecond (fs) laser ablation, also referred to as ultrafast laser ablation, is gaining popularity in micromanufacturing and texturing applications due to its high flexibility and accuracy. However, the non-linear nature of the process complicates the task of finding the right laser parameters and laser strategy for a desired geometry. As a result, researchers and operators often rely on long and costly trial and error before they find the optimal process parameters. Predictive models can shorten this process significantly. Chichkov et al. [1] introduced a two-temperature model describing the evolution of the temperature of the electrons and the lattice during ultrashort pulse ablation. This model leads to the following equation describing the ablation depth z for pulses shorter than the electron-phonon relaxation time:

$$z = \delta * \ln \left(\frac{F}{F_{th}} \right) \quad (1)$$

where F is the laser fluence, F_{th} the threshold fluence and δ the penetration depth of electromagnetic waves into the target material. Important to note is that the penetration depth δ is inversely proportional to the extinction coefficient κ , where κ is defined as the imaginary part of the refractive index of the target material. The threshold fluence is defined as the minimum fluence needed for ablation. For a low number of pulses, F_{th} and δ are described by the following equations:

$$F_{th}(N) = F_{th}(1) * N^{S-1} \quad (2)$$

$$\delta(N) = \delta(1) * N^{S-1} \quad (3)$$

with N the number of pulses and S the incubation factor, usually equal to 0.8 for metals [2]. For a high number of pulses

($N > 20$), F_{th} and δ become constant and equal to $F_{th}(> 20)$ and $\delta(> 20)$, respectively.

Cangueiro et al. [3] presented a two-dimensional approach based on the two-temperature model for high aspect ratio features. This approach includes the angle of incidence dependent reflectivity and a correction factor taking into account the local fluence. The authors validated their model using a plane-polarized beam, a fixed value for δ , and they performed exclusively line scanning experiments.

In this work, the two-temperature model will be used in combination with the reflectivity and fluence corrections presented in [3] for percussion drilling experiments with circular polarization.

2. Materials and methods

2.1. Materials

A low corrosion tool steel (grade 1.2083, soft annealed to approx. 190 HB) was used as target material for the fs laser percussion drilling experiments. The 20 mm thick sample was first grinded and then polished with a 6 μ m diamond paste. The low corrosion tool steel is assumed to have similar optical and thermal properties as stainless steel (AISI 316L), which has been more widely studied and referenced in the scientific literature. The constants describing the behaviour of the material during fs laser ablation as found in databases and scientific literature are given in Table 1. After the laser ablation process, the plate thickness was reduced to 2 mm to improve the sensitivity of the μ -CT detector (see Section 2.3).

Table 1. Material properties of stainless steel.

Threshold fluence	$F_{th}(1)$ [4]	0.1001 J/cm ²
	$F_{th}(> 20)$ [4]	0.055 J/cm ²
Complex refractive index	κ [5]	4.49
	n [5]	3.81
Penetration depth	$\delta(1)$ [4]	32.77 nm
	$\delta(> 20)$ [4]	18.00 nm
Incubation factor	S [2]	0.8

2.2. Laser machining

Four experiments were performed to assess the validity of the fs laser ablation model with different numbers of pulses. Each experiment was repeated three times to average material inhomogeneities and laser instabilities. A Lasea LS5 machine equipped with a Satsuma HP femtosecond laser from Amplitude Systems was used to perform these experiments. This laser generates a beam with gaussian profile at 1030 nm wavelength and circular polarization. The maximum average power delivered on target is 7.7 W, and the pulse length is 250 fs. The repetition rate was kept at 500 kHz for the entirety of the experiments, and the power was kept at the maximum. The beam focus radius is 8.2 μm . For the experiments, the number of pulses was varied between 2000 and 5000 in steps of 1000 pulses. The percussion drilled holes were separated by 2 mm to prevent any interaction between craters.

2.3. Topography characterization

Micro-CT was used to characterize the craters. The $\mu\text{-CT}$ system (Phoenix Nanotom) consisted of a diamond target, a 0.1 mm thick Cu-Zn filter, and a nanofocus X-ray tube. The top 2 mm of the lasered plate were first separated from the bulk with wire-EDM, then this thin plate was cut into strips of 2 mm wide and approximately 20 mm long. Each strip included four craters. Each scan consisted of 2400 images and was taken with the “fast-scan” function active. The acquisition parameters were: current = 80 μA , voltage = 120 V, voxel size = 1.5 μm . GE phoenix datos|x REC was used as reconstruction software to generate slices, and the slices were analysed with Fiji ImageJ. Figure 1 shows a slice of a percussion drilled crater.

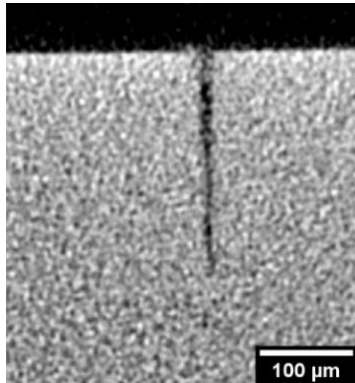


Figure 1. Reconstructed $\mu\text{-CT}$ slice of a percussion drilled crater. Black = air, grey = steel.

3. Results and discussion

The depths of the percussion drilled craters were first compared to the depths of the simulation results with the constants from the literature (see Table 1). Afterwards, the extinction coefficient was slightly modified to achieve a better fit for the penetration depth as is shown in Figure 1.

It can be observed from Figure 1 that the original simulation results underestimate the final crater depths for all numbers of pulses, except for the 5000 pulses crater. This point shows a sudden decrease in the growth of the crater above 4000 pulses. This decrease can possibly be due to the saturation phenomenon for high aspect ratio features mentioned by Nasrollahi et al. (2018) [6] and Audouard et al. (2016) [4].

However, it should be confirmed by experiments at higher number of pulses. The average error on the depth is 7 %. To compensate for this error, the imaginary part of the complex refraction index, also called the extinction coefficient, can be lowered. This has a direct influence on the two following phenomena: (i) the reflectivity decreases, meaning that more energy is used for ablation, and (ii) the penetration depth, which is inversely proportional to the extinction coefficient, increases, which results in a higher ablation depth. An improved fit is found for $\kappa = 4.0$ instead of 4.49. The penetration depths are modified according to the inverse proportionality between δ and κ , and become $\delta(1) = 37.31$ nm and $\delta(> 20) = 20.49$ nm. The results of the simulations with optimized extinction coefficient are also shown in Figure 2 and have a better fit with the experimental crater depths. The average error on the depth is decreased to 1 %, but the error on the last point (5000 pulses) increased, which could be due to the already discussed saturation phenomenon.

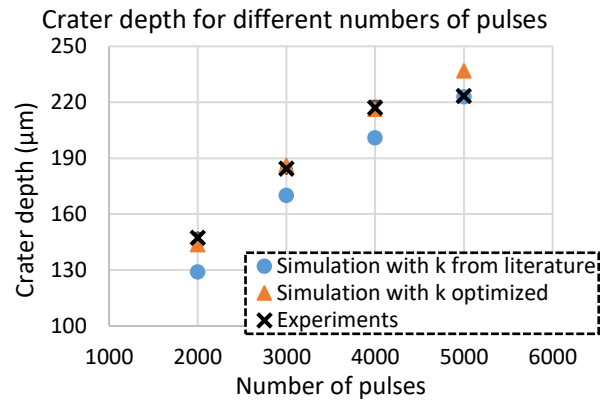


Figure 2. Percussion drilled crater depths for varying numbers of pulses. The error bars represent the standard error of the mean (SEM).

4. Conclusion

In this work, the validation of a two-dimensional approach for the modelling of percussion drilled laser ablated holes is presented. The simulations show a good correspondence with the experimental values after optimization of the extinction coefficient: the average error on the depth is 1%. Further research is necessary to prove the saturation at higher number of pulses, and eventually adapt the model accordingly. Also, this model should allow the simulation of more complicated laser strategies, but would require modifications for the implementation of three-dimensional laser strategies.

Acknowledgements: This research was supported by Internal Funds KU Leuven through the interdisciplinary network project IDN/20/011—MIRACLE. The FWO large infrastructure I013518N project is acknowledged for the financial support of the X-ray infrastructure and the KU Leuven XCT Core facility is acknowledged for the 3D image acquisition and quantitative post-processing tools (<https://xct.kuleuven.be/>).

References

- [1] Chichkov B N, Momma C, Nolte S, Von Alvensleben F and Tünnermann A 1996 *Appl. Phys. A* **63** no. 2 pp. 109–15
- [2] Di Niso F, Gaudio C, Sibillano T, Mezzapesa F P, Ancona A and Lugarà P M 2014 *Opt. Express*, **22**, no. 10 p. 12200
- [3] Cangueiro L et al. 2018 Proc. of SPIE vol. **10520** p. 38.
- [4] Audouard E and Mottay E 2016 *Frontiers in Ultrafast Optics: Biomedical, Scientific, and Industrial Applications XVI* **9740** p. 974016
- [5] Steen W M and Mazumder J 2010 *Laser Material Processing* 4th ed. 20. London: Springer London : Imprint: Springer p. 90
- [6] Nasrollahi V, Penchev P, Jwad T, Dimov S, Kim K and Im C 2018 *Opt. Lasers Eng.* **110** pp. 315–22